The 8th European Congress on Computational Methods in Applied Sciences and Engineering
ECCOMAS Congress 2022
5--9 June 2022, Oslo, Norway

MATHEMATICAL MODELING AND NUMERICAL RESULTS ON THE PROPAGATION OF SOLITARY WAVES ON TENSEGRITY LATTICES

ADA AMENDOLA[1], FERNANDO FRATERNALI[1], GIUSEPPE SACCOMANDI[2,3]

[1]Department of Civil Engineering, University of Salerno, Fisciano (SA), Italy.
[2]Dipartimento di Ingegneria e Sezione INFN di Perugia, Università degli Studi di Perugia, 06125 Perugia, Italy.
[3]School of Mathematics, Statistics and Applied Mathematics, NUI Galway, University Road, Galway, Ireland.

Key words: Tensegrity, Prestress, Compact compression waves, Wave profile

Abstract. This work discusses the mathematical properties of the interaction potential that characterizes tensegrity mass-spring chains, and its implications in terms of the propagation of compact compression waves in such systems when impacted by a striker. Numerical simulations show evidence of the dependence of the wave form on the speed of the propagating compression pulses, which change shape when passing from the sonic to the super-sonic wave propagation regime.

1 Introduction

Most of the currently available methods for the focusing and defocusing of acoustic waves, based mostly on exploiting linear acoustic phenomena, present the problem of having essentially small tunability ranges and poorly scalable dimensions [1]. Available literature studies have shown that the employment of nonlinear acoustic systems, which permit a high level of control of the propagation of mechanical waves over the wave speed, may enable the creation of novel types of acoustic lenses with more advanced wave-focusing methodologies [2, 3, 4]. The present study discusses the design of one-dimensional tensegrity metamaterials featuring elastically stiffening (or hardening) response for the fabrication of novel acoustic lenses and structural health monitoring devices [5, 6, 7, 8, 9]. We mathematically characterize the interaction potential of chains alternating tensegrity prisms, acting as nonlinear springs, and lumped masses. Next, we numerically show the existence of compression waves with compact support in such systems, under suitable conditions on the propagation velocity. The examined pulses exhibit atomic scale localization in the super-sonic regime, which proves to be useful for building actuators that are able to focus mechanical waves in small targeted areas of host media.

2 Chains of tensegrity prisms

Let us consider a structure that consists of an array of discs connected each other by minimal regular tensegrity prisms. The i-th unit is built using two discs (the end faces) $\mathcal{D}_i$ and $\mathcal{D}_{i+1}$, three uniform rigid bars of length L, and three diagonal cross-cables, of identically length and linearly elastic stiffness k (Fig. 1). The end points of the top base of the i-th prism are in contact without friction with $\mathcal{D}_i$, while the end points of the bottom base are in contact without friction with to $\mathcal{D}_{i+1}$, in such a way that they form two equilateral triangles, and the two discs are perpendicular to the axis joining the centroids of the triangles (Fig. 1). Such triangles are twisted by a an angle ϕ one another. We assume that these elements of the prisms transform rigidly during the motion of the system, as well as the bars, while the cross-strings deform elastically (rigid-elastic model, see also [5, 6, 7]). The contact without friction between the prisms and the discs ensures that that no bending moments and torques are transmitted from the prisms to the discs. We also assume that the tensegrity prisms are much lighter than the spacing discs, which are modeled as point masses where the overall mass of the units is lumped [7, 8]. The model shown in Fig. 1 features 300 prisms featuring bars made of carbon hollow tubes (external diameter 4 mm; internal diameter 2.54 mm; length $L = 180$ mm); cross-cables with diameter of 2 mm made of a Nylon 6 with Young modulus of 1800 MPa; 140 mm diameter polycarbonate disks with thickness of 1.57 mm; and a total mass $m = 35$ g.

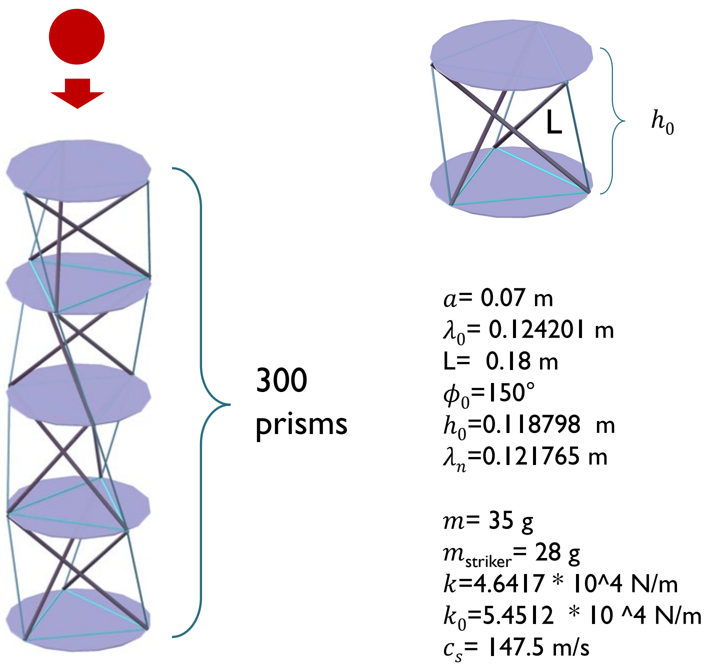

Figure 1: One-dimensional array of tensegrity units and lumped masses forming a nonlinear mass-spring chain subject to impact loading.

{chain}

With some simple computations it is possible to compute that the prism height, h, is given by [7]

$$h(\phi) = \sqrt{L^2 - 2\alpha^2[1 - \cos(\phi)]}, \tag{1}$$ {i1}

where α is the distance between the centroid of the triangle and its vertices, and it results

$$h(\pi) \equiv \sqrt{L^2 - 4\alpha^2} \leq h(\phi) \leq h(0) \equiv L,$$

We point out that $\phi \in [-\pi/3, \pi]$. Computing the cross-cable length as

$$\lambda = \sqrt{L^3 + 3\alpha^2 \cos(\phi) - \sqrt{3}\alpha^2 \sin(\phi)}, \tag{2}$$ {i2}

the elastic potential associated with the three cables is given by

$$U = \frac{3}{2}k(\lambda - \lambda_n)^2, \tag{3}$$ {i3}

where λ_n is the length at zero stress. Clearly, the axial force F acting on the prism (positive in compression) is given by $F = -dU/dh = -3k(\lambda - \lambda_n) d\lambda/dh$. When $F = 0$ we recover the tensegrity placement and this occurs only for the special value of the twist angle $\phi_0 = 5/6\pi$, in correspondence of which we have

$$h_0 = \sqrt{L^2 - (2+\sqrt{3})\alpha^2}, \quad \lambda_0 = \sqrt{L^2 - 2\sqrt{3}\alpha^2}.$$

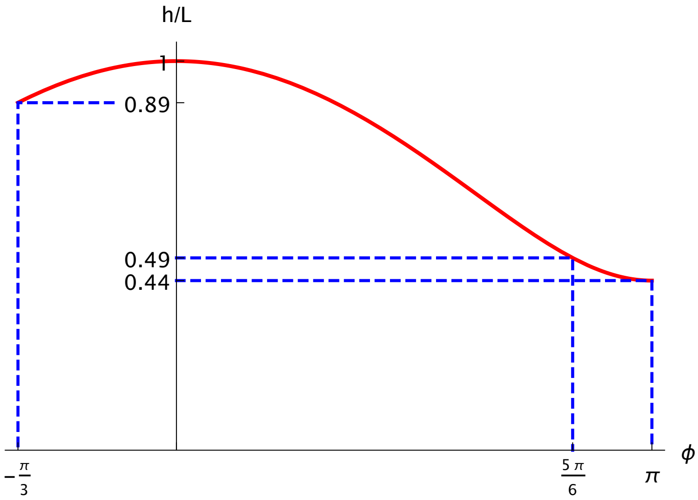

Figure 2: Plot of the law relating the dimensionless prism height h/L to the twist angle ϕ, for $\alpha/L = 0.45$.

{hphilaw}

The positive quantity

$$p = \frac{\lambda_0 - \lambda_n}{\lambda_n},$$

is the prestrain of the cross-cables. Let us introduce the relative axial displacement $r = h - h_0$. Clearly $r_m = h(\pi) - h_0 < 0$ and $r_M = h(0) - h_0 > 0$. Then it is possible to introduce the positive axial strain

$$\epsilon = \frac{h_0 - h}{h_0},$$

and introducing the dimensionless quantities $\tilde{\alpha} = \alpha/h_0$, $\tilde{L} = L/h_0$, and $\tilde{\lambda}_0 = \lambda_0/h_0$ we consider that $\epsilon \in [\epsilon_-, \epsilon_+]$ where

$$\epsilon_+ = \frac{h_0 - h(\pi)}{h_0} \equiv 1 - \sqrt{\tilde{L}^2 - 4\tilde{\alpha}^2}, \quad \epsilon_- = \frac{h_0 - h(0)}{h_0} \equiv 1 - \tilde{L}.$$

We also introduce the quantity

$$\mathcal{C}(\epsilon) = \frac{1}{\tilde{\alpha}^2}\sqrt{[\tilde{L}^2 - (1-\epsilon)^2][4\tilde{\alpha}^2 + (1-\epsilon)^2 - \tilde{L}^2]},$$

and collecting all the above details we write

$$\tilde{U}(\epsilon) \equiv \frac{2}{3h_0^2 k} U(\epsilon) = \left[\frac{1}{\sqrt{2}}\sqrt{3(1-\epsilon)^2 - \tilde{L}^2 + \tilde{\alpha}^2(6 - \sqrt{3}\mathcal{C})} - \frac{\tilde{\lambda}_0}{1+p}\right]^2 \tag{4}$$ {i4}

It is easily verified that the prism in Fig. 1 is characterized by the $U - U_0$ vs. ϵ law ($U_0 = U(\epsilon = 0)$ denoting the elastic potential associated with the prestrain of the cross-cables), and the F vs. ϵ law that are displayed in Fig. 3 (we have assumed $p = 2\%$). Such a prism shows a locking strain $\epsilon_+ = 4.76\%$, an initial axial stiffness $k_0 = 5.412 \times 10^4$ N/m, and a speed of sound in the linear regime $c_s = 147.5$ m/s (see [7] for further details). The plots given in Fig. 3 highlight a locking response of the prism for $\epsilon \to \epsilon_+$, which originates the phenomenon of wave propagation through compact compression waves that is discussed in the following section.

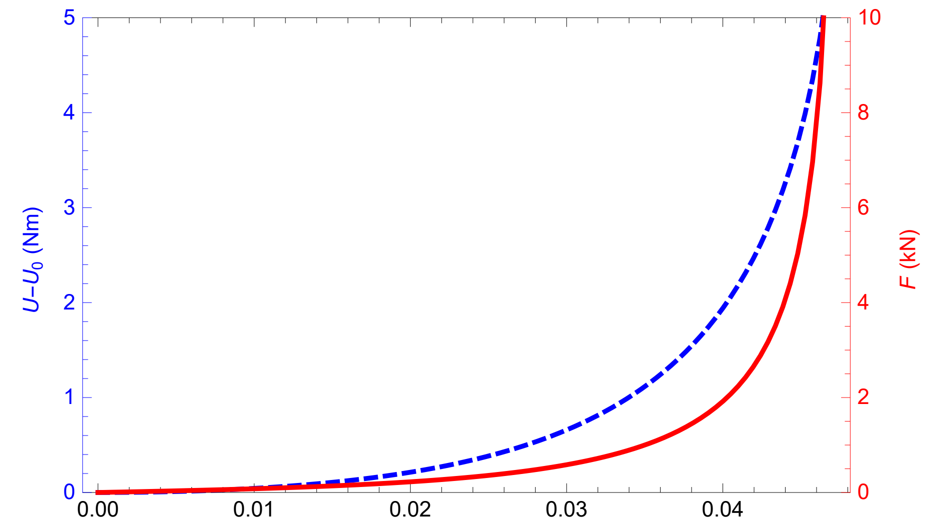

Figure 3: Illustration of the U vs. ϵ and law (dashed blue curve) and the F vs. ϵ law (solid red curve) characterizing the response of the tensegrity prism shown in Fig. 1 under compression loading.

{figFU}

3 Propagation of compact compression waves

We now numerically study the propagation of compression waves along the system shown in Fig. 1, due to the impact of a 28 g mass striker. The striker is given different impact velocities, so as to generate waves travelling with different speeds through the chain. The equations of motion of the system are numerically solved through a Runge-Kutta explicit integration scheme with a time integration step of 10^{-8} s. The results presented hereafter complement those illustrated in Ref. [7], to which we address the reader for further details.

Let V_s denote the speed of the peak of the compact compression wave that is generated due to the impact loading. Fig. 4 shows the profiles of strain and stress (axial forces) waves recorded at the steady state in the system under examination, for various values of V_s. In these plots, x denotes the longitudinal coordinate centered at the peak of the pulse. The examined compression waves include pulses propagating at a nearly sonic speed (V_s close to the sound of speed in the linearized system: $c_s = 147.5$ m/s), and supersonic waves (V_s up to 500 m/s). The results shown in Fig. 4 point out that the traveling compression pulses nearly have a bell shape in the sonic regime, and tend to localize in a single unit for $V_s \gg c_s$. A mathematical discussion about the solitary wave nature of such pulses is given in [7, 10].

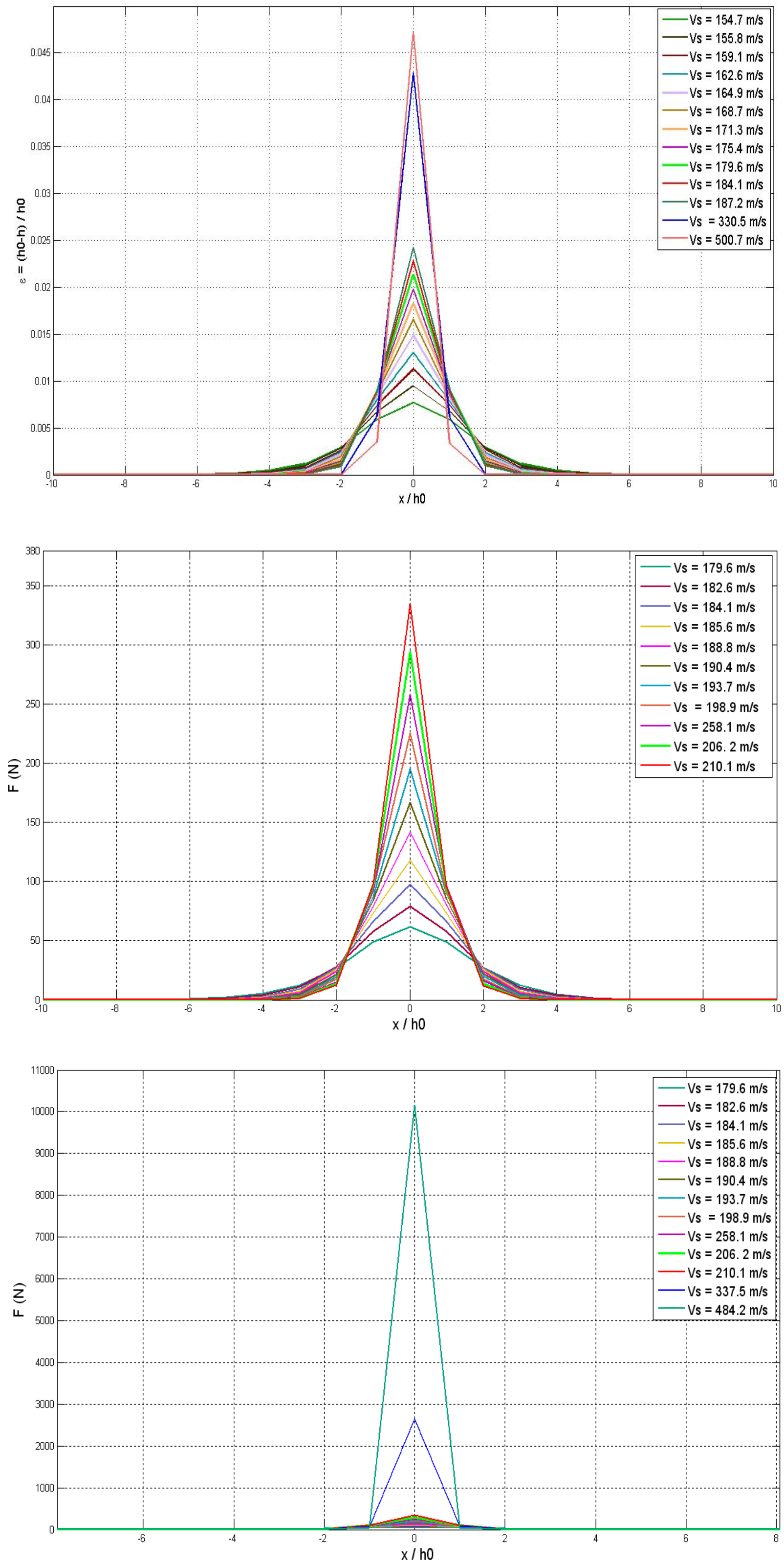

Figure 4: Profiles of strain and stress (axial force) waves propagating through the system shown in Fig. 1, in correspondence with different values of the traveling speed V_s.

{fig5}

4 Concluding Remarks

We have examined the propagation of compression waves with compact support in chains of tensegrity prisms alternating with lumped masses. A numerical study has confirmed previous literature results on the wave dynamics of tensegrity mass-spring chains exhibiting locking behavior in compression [7, 8]. Such a dynamic response can be exploited to design tensegrity acoustic lenses and/or sensor-actuators for the focusing of mechanical waves in host media [11]. We address this study, as well as the employment of the Weinstrass theory for the mathematical analysis of the compact compression waves supported by the examined systems [12], to future work.

REFERENCES

[1] Yang, S.X., et al., 2004. Focusing of sound in a 3-D phononic crystal. Phys Rev Lett, 93(2).

[2] Daraio, C., et al., 2006. Tunability of solitary wave properties in one-dimensional strongly nonlinear phononic crystals. Phys Rev E, 73(2).

[3] Spadoni, A. and Daraio, C., 2010. Generation and control of sound bullets with a nonlinear acoustic lens. Proc. Natl. Acad. Sci. U.S.A. 107(16), 7230-7234.

[4] Donahue, C., Anzel, P., Bonanomi, L., Keller, T.; Daraio, C., 2014. Experimental realization of a nonlinear acoustic lens with a tunable focus, Appl Phys Lett, 104, 014103

[5] Oppenheim, I. J., & Williams, W. O. (2000). Geometric effects in an elastic tensegrity structure. Journal of Elasticity, 59(1-3), 51-65.

[6] Oppenheim, I. J., & Williams, W. O. (2001). Vibration of an elastic tensegrity structure. European Journal of Mechanics-A/Solids, 20(6), 1023-1031.

[7] Fraternali, F., Senatore, L. and Daraio, C., 2012. Solitary waves on tensegrity lattices. J Mech Phys Solids 60, 1137-1144.

[8] Fraternali, F., Carpentieri, G., Amendola, A., Skelton, R.E., Nesterenko, V. F., 2014. Multiscale tunability of solitary wave dynamics in tensegrity metamaterials. Appl Phys Lett, 105, 201903.

[9] Micheletti, A., Ruscica, G., Fraternali F., 2019. On the compact wave dynamics of tensegrity beams in multiple dimensions. Nonlin Dyn, 98, 2737–2753.

[10] Friesecke, G. and Matthies, K. (2002). Atomic-scale localization of high-energy solitary waves on lattices. *Physica D*, 171:211–220.

[11] Daraio, C., Fraternali, F. 2013. "Method and apparatus for wave generation and detection using tensegrity structures," US Pat. No. 8,616,328, granted on December 31, 2013.

[12] Destrade, M., Gaeta, G., & Saccomandi, G. (2007). Weierstrass's criterion and compact solitary waves. Physical Review E, 75(4), 047601.